BioResearch Open Access
Volume 3, Number 5, October 2014

DOI: 10.1089/biores.2014.0023

Contribution of Fibroblasts to the Mechanical Stability of *In Vitro* Engineered Dermal-Like Tissue Through Extracellular Matrix Deposition

Renjith P. Nair,[1] Jasmin Joseph,[2] V.S. Harikrishnan,[3] V.K. Krishnan,[2] and Lissy Krishnan[1]

Abstract

Tissue-engineered skin with mechanical and biological properties that match the native tissue could be a valuable graft to treat non-healing chronic wounds. Fibroblasts grown on a suitable biodegradable scaffold are a feasible strategy for the development of a dermal substitute above which epithelialization may occur naturally. Cell growth and phenotype maintenance are crucial to ensure the functional status of engineered tissue. In this study, an electrospun biodegradable polymer scaffold composed of a terpolymer PLGC [poly(lactide-glycolide-caprolactone)] with appropriate mechanical strength was used as a scaffold so that undesirable contraction of the wound could be prevented when it was implanted. To enhance cell growth, synthetic PLGC was incorporated with a fibrin-based biomimetic composite. The efficacy of the hybrid scaffold was evaluated by comparing it with bare PLGC in terms of fibroblast growth potential, extracellular matrix (ECM) deposition, polymer degradation, and mechanical strength. A significant increase was observed in fibroblast attachment, proliferation, and deposition of ECM proteins such as collagen and elastin in the hybrid scaffold. After growing fibroblasts for 20 d and 40 d, immunochemical staining of the decellularized scaffolds showed deposition of insoluble collagen and elastin on the hybrid scaffold but not on the bare scaffold. The loss of mechanical strength consequent to *in vitro* polymer degradation seemed to be balanced owing to the ECM deposition. Thus, tensile strength and elongation were better when cells were grown on the hybrid scaffold rather than the bare samples immersed in culture medium. Similar patterns of *in vivo* and *in vitro* degradation were observed during subcutaneous implantation and fibroblast culture, respectively. We therefore postulate that a hybrid scaffold comprising PLGC and fibrin is a potential candidate for the engineering of dermal tissue to be used in the regeneration of chronic wounds.

Key words: skin tissue engineering; dermal substitute; biodegradable scaffold; tissue equivalent; extra cellular matrix deposition; mechanical strength

Introduction

FULL-THICKNESS CHRONIC skin wounds result in extensive scarring and severe cosmetic deformities and require skin grafting.[1] The use of natural skin substitutes such as allografts, xenografts, and autografts face risk of infection, immune rejection, donor site morbidity, and scar formation. Tissue engineering is considered an alternative approach for treating such skin wounds.[2]

Several natural and synthetic polymeric biomaterials have been used as scaffolds in skin tissue engineering to guide and support cell growth.[2–5] Natural polymers possess biological cues for cell recognition and proliferation.[6,7] However, poor mechanical strength and faster degradation are major limitations,[4] leading to wound contraction, deformation, and scarring. Therefore, a synthetic polymer with appropriate mechanical strength and degradation rate could be a viable alternative. For skin tissue engineering, bioabsorbable polyesters comprising glycolide (GA)/lactide (LA)/ε-caprolactone are preferred as they are biocompatible and approved by the U.S. Food and Drug Administration. Poor cell growth on synthetic polymers is a limitation, and this may be countered by combining natural polymers such as collagen, chitosan, gelatin, fibronectin, and fibrin.[8–11] Fibrin-based biomimetic composites have been used to grow endothelial cells on various biomaterials for vascular tissue engineering applications.[11,12] Fibrin is a biocompatible and biodegradable material that is less immunogenic than other biological matrices

[1]Thrombosis Research Unit, [2]Dental Products Laboratory, and [3]Division of Laboratory Animal Science, Biomedical Technology Wing, Sree Chitra Tirunal Institute for Medical Sciences and Technology, Trivandrum, India.

of nonhuman origin and it is being widely used as a sealant and drug delivery vehicle.[13] In physiology, the fibrin clot is the natural scaffold for cell migration and wound healing.[14] Hyaluronic acid (HA) is also useful because it is an important constituent of the natural extra cellular matrix (ECM) of skin and its beneficial role in wound healing has been reported.[15]

Electrospinning has emerged as an efficient technique to generate nano- and micro-architectural fibers similar to the fibrous structures of native ECM.[16] By manipulating spinning conditions, parameters like evaporative water loss, oxygen permeability, and fluid drainage ability due to porosity can be controlled.[17,18]

For the current study, it was hypothesized that a biomimetic fibrin composite matrix (fibrin-HA) immobilized on the electrospun terpolymer PLGC [poly(lactide-glycolide-caprolactone)] may enhance tissue generation, and more specifically, ECM production. The objective was to establish the contribution of cell growth and ECM deposition to the mechanical stability of the hybrid scaffold as compared with the bare PLGC scaffold.

Materials and Methods

Scaffold fabrication

The terpolymer PLGC was synthesized using a reported procedure[19] with a starting monomer (Sigma Chemicals) ratio of 70:10:20. For electrospinning, a well-characterized (data not shown) polymer solution (15% w/w) in dichloromethane was fed using a syringe pump (Holmarc Opto-Mechatronics Pvt. Ltd) at a flow rate of 3 mL/hour, and a voltage of 11 kV was applied (Zeonics Systech Defence and Aerospace Engineers Ltd.) to collect the fibers. The electrospun fiber matrices were dried under vacuum at room temperature for 24 hours, cut into patches of the required size for each experiment, and sterilized using ethylene oxide.

The biomimetic fibrin composite matrix was deposited on the polymer as described earlier.[11] The biomimetic matrix comprised cryoprecipitated human fibrinogen concentrate (10 mg/mL) and HA (50 μg/mL) prepared in-house as described previously.[15] Briefly, 100 μL/cm^2 fibrin composite was layered on a sterile, thrombin-adsorbed scaffold, incubated for 30 min at 37°C, lyophilized (Edwards, Modulyo 4K), and stored at 4°C–6°C until use.

Analysis of scaffolds

The spectra of the scaffold and its components were recorded using a JASCO FT-IR Spectrometer 6300 (Japan) by the attenuated total reflectance method. The morphology of the bare and hybrid scaffolds was analyzed by environmental scanning electron microscopy (ESEM, FEI Quanta 200) and bright field microscopy (Leica).

Water vapor transmission rate (WVTR) was measured by gravimetric methods.[16] Briefly, the scaffold sheet was firmly secured over the mouth of the water-filled evaporating dish; weight was noted immediately and after incubation of the dish at 37°C under 50% humidity for 3 d. The weight loss was plotted against the elapsed time to get a slope (reduction in grams per day). To calculate the WVTR, the slope was divided by the area of the mouth of the dish. WVTR = [slope (g/d)] / [test area (m^2)].

Swelling property was analyzed gravimetrically. Pieces of dry, bare/hybrid scaffolds were weighed (W_d), immersed in petri dishes containing phosphate buffered saline (PBS;pH 7.4), and placed in an incubator at 37°C for 24 h. After blotting off the excess water, the swollen scaffolds were weighed (Ws). Percentage of swelling = $[(W\text{s} - W_d) / W_d] \times 100$.

In vitro *cell growth on scaffolds*

Unidentifiable foreskin discarded from circumcision was collected from a local hospital with informed consent as required by the ethics committee of the organization. After thorough washing in Hanks' Balanced Salt Solution (HBSS) with an antibiotic-antimycotic (Gibco), fat and loose fascia were trimmed off, and tissue pieces of size $\sim$2 mm $\times$ 2 mm were placed with the dermal side in contact with the culture surface for explant outgrowth. The tissue was overlaid with $\sim$ 100 μL Dulbecco's modified Eagle medium : F12 medium (Gibco) containing 10% FBS (Gibco). In $\sim$10 days, the sprouted cells were harvested by standard trypsin digestion and subcultured at 1:3 split ratio. Fibroblasts harvested from the fourth passage were used for seeding on scaffolds. Test and control scaffolds were seeded with fibroblasts at a seeding density of 2×10^4 cells/cm. Replicate strips of size 1 cm $\times$ 5 cm and patches 1 cm in diameter were used for mechanical testing and analysis of other growth parameters, respectively. The medium was changed every third day and the culture was terminated after specific periods for each analysis.

Analysis of cell-grown scaffolds

After 7 d/28 d, the cells on the scaffolds were viewed and imaged using an environmental scanning electron microscope (ESEM, FEI Quanta 200). For actin identification, the cell-grown scaffolds were fixed with 3.7% formaldehyde and permeated by 0.2% triton $\times$ 100 and then stained with Texas Red Phalloidin (Molecular Probes; 1:250) for 45 min. The cells were counterstained with Hoechst (Sigma) for 10 min and imaged using a fluorescent microscope (Leica, DMIRB) and confocal microscope (Carl Zeiss LSM 510 Meta). Projection images (Z-stack) were created from 30 XY images taken at 1.5-μm intervals. Quantification of fibroblast adhesion and proliferation on the bare and hybrid scaffolds was carried out using the ^{3}H-thymidine (American Radiochemicals) uptake assay.[21]

Analysis of scaffolds after cell culture

The tensile strength and percentage of elongation at break were analyzed using a Universal Testing Machine (Instron 1011) at a crosshead speed of 20 mm/min. The coated PLGC scaffold strips incubated without fibroblasts in similar culture conditions for 20 d and 40 d were included as controls to compare degradation in the absence of cells. The test (cell-grown) and control scaffolds were minced and dissolved in tetrahydrofuran (THF; Merck), centrifuged, and subjected to gel permeation chromatography (GPC) using the Waters high-performance liquid chromatography system with 600 series pump. Mobile phase was THF at a flow rate of 1 mL/min. The changes in number average (Mn) and weight average (Mw) molecular weights were determined.

The cells grown on the scaffolds were removed using a modified hypotonic-alkaline-detergent-treatment method.[21] The

scaffolds were then washed three times with PBS and fixed with 3.7% formaldehyde for 30 min before washing again with PBS. The decellularized scaffolds were immunostained for collagen and elastin using monoclonal antibodies (1:1000 dil; Novocastra) after blocking with 1% BSA (Sigma) for 30 min. Bound primary antibodies were developed using Texas Red conjugated secondary antibodies (Abcam) and imaged using a fluorescent microscope (Leica, DMIRB).

The assay to determine the collagen content in the decellularized PLGC scaffold was carried out using sirius red according to published protocols.[22] The absorbance of the extracted collagen–sirius red complex was measured in a 96-well plate at 540 nm using a microplate reader (Asys UVM340 Microplate Reader). The concentration of collagen deposited on the scaffold was estimated using calibration standards made from type 2 collagen (bovine achilles tendon, Sigma). The soluble elastin content on the decellularized scaffold was quantified using a Fastin elastin assay kit (Biocolor) according to the manufacturer's instructions. The elastin deposited was estimated using calibration standards supplied with the kit.

In vivo *degradation of scaffold*

Scaffold patches were implanted in subcutaneous tissue of rabbit skin. All animal procedures were conducted with permission from the Institutional Animal Ethics Committee as

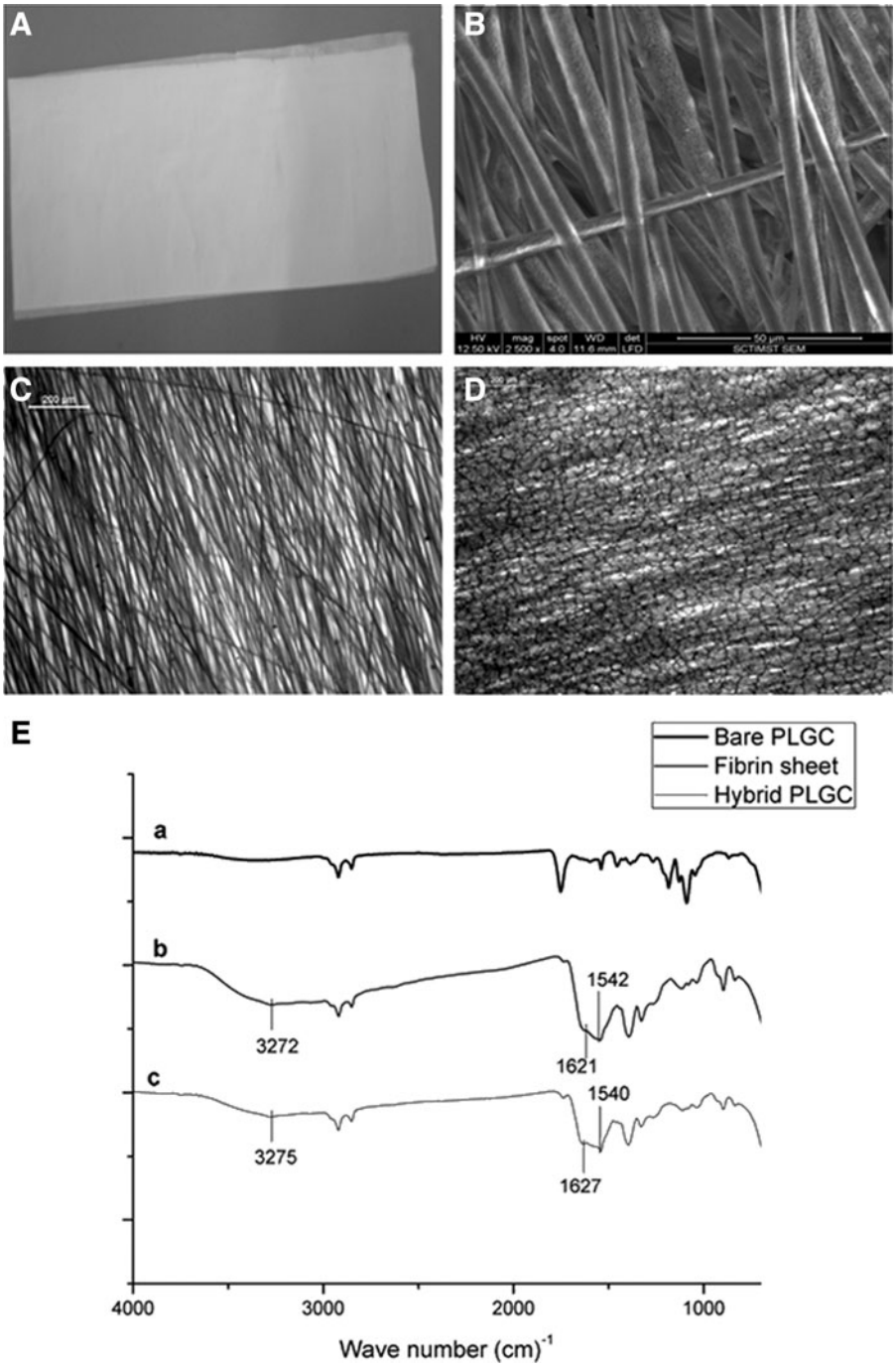

FIG. 1. Representative images of the scaffolds. **(A)** Gross image of electro spun poly(lactide-glycolide-caprolactone) (PLGC). **(B)** Environmental scanning electron microscopy (ESEM) image of bare PLGC. **(C)** Bright field micrographs of bare PLGC. **(D)** Bright field micrographs of hybrid PLGC showing fibrin network. **(E)** Merged attenuated total reflectance-infrared spectroscopy of (*a*), bare PLGC scaffold, (*b*) fibrin composite matrix sheet, and (*c*) hybrid PLGC scaffold. Spectral recording of hybrid scaffold shows characteristic peaks of O-H stretching, amide 1 band and amide 2 band at 3275 cm^{-1}, 1627 cm^{-1}, and 1540cm^{-1}, respectively which is seen in the spectrum of fibrin composite. These peaks are absent in the spectrum of bare PLGC.

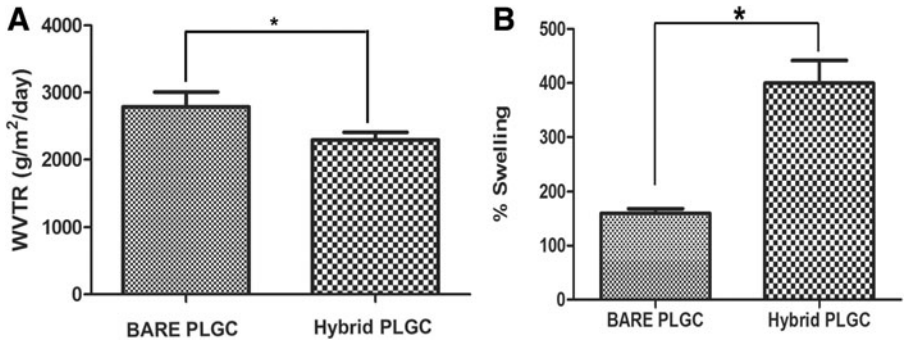

FIG. 2. Physical properties of porous scaffold. **(A)** Comparison of water vapor transmission rate of the bare and hybrid scaffolds. **(B)** Comparison of swelling percentage of the bare and hybrid scaffolds. The water vapor transmission rate of the bare PLGC and the hybrid PLGC are in the same range with values of $2789 \pm 220 \cdot gm^{-2} \cdot d^{-1}$ and $2295 \pm 111\, g \cdot m^{-2} \cdot d^{-1}$, respectively. The transmission has reduced significantly upon the fibrin matrix deposition but both values are in the same range required. For each parameter, data from replicate experiment was compiled and average ± standard deviation (SD) ($n = 4$) are shown. $^*p < 0.05$.

per Committee for the Purpose of Control and Supervision on Experiments on Animals (CPCSEA) (Government of India) guidelines. Young adult New Zealand white rabbits with an average weight of 2.47 ± 0.17 kg were used for the study. Briefly, the rabbits were anaesthetized with ketamine hydrochloride (50 mg/kg) and xylazine (5 mg/kg). Subcutaneous pockets were created in the rabbit's skin and PLGC scaffolds were implanted in the pockets. The wound was closed with 3-0 braided silk sutures in a simple interrupted pattern. The animals were housed and cared for under standard environmental conditions as per International Standard ISO10993 part 2 and CPCSEA guidelines. After specific time periods (20 d and 40 d), the rabbits were euthanized with an overdose of an intravenous injection of 1% thiopentone sodium and the scaffolds were harvested. The explanted tissues with scaffolds were minced into small pieces with a surgical scalpel blade and dissolved in the solvent, and the cleared extract was subjected to GPC analysis as described for *in vitro* degradation analysis.

Statistical analysis

For each test, more than three replicate experiments were carried out and average standard deviation was calculated. The difference in scores among the groups was analyzed using the Student's t test and considered significant when $p < 0.05$. The number of samples used for each experiment is indicated in the legend for each figure.

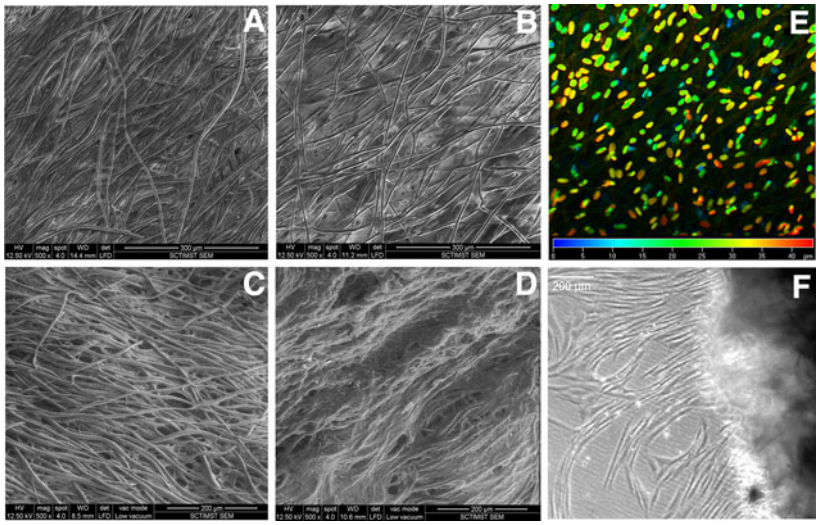

FIG. 3. Representative micrographs of fibroblast growth on scaffolds. **(A, B)** ESEM images of fibroblast cultured for 7 d on bare PLGC and hybrid scaffold, respectively. **(C, D)** ESEM images of fibroblast cultured for 28 d on bare PLGC and hybrid scaffold, respectively. The inter fiber space of bare scaffold appeared empty and the cells appeared to have grown along the fibers but the fibers of hybrid scaffold were connected by cell sheets. **(E)** Confocal image of scaffold after nuclear stain; color code indicates Z-depth of cells inside the hybrid scaffold after 7 d of fibroblast culture. **(F)** Light micrograph of 28-d-old construct with migratory fibroblasts; cell sprouting seen is 24 h after transfer into an empty dish. Scale bars: 300 μm **(A, B)**; 200 μm **(C, D)**; and 200 μm **(F)**.

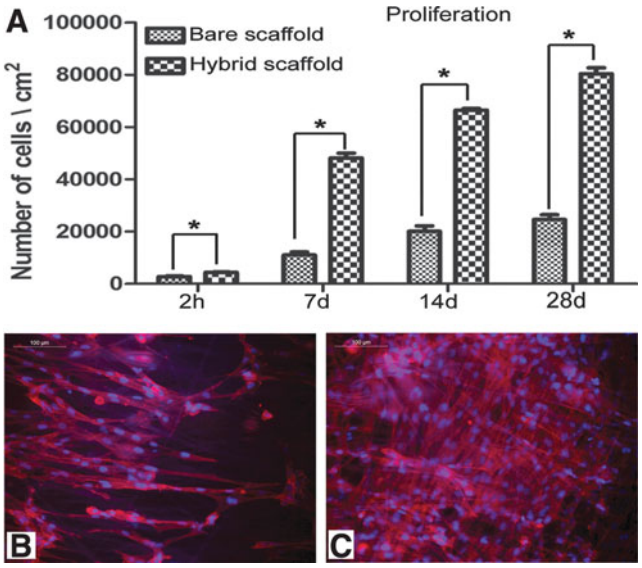

FIG. 4. Evidence for cell proliferation on scaffolds. **(A)** Data on ^{3}H-thymidine uptake assay. The adhesion of fibroblasts on bare PLGC and hybrid PLGC scaffolds within 2 h and proliferated cell numbers after 7 d, 14 d, and 28 d of culture are shown graphically. Bars represent mean ± SD, ($n = 3$). *$p < 0.05$. **(B, C)** Micrograph of actin-stained cytoskeleton, counter stained with Hoechst for nucleus of fibroblast after 7 d of culture on bare PLGC scaffold and on hybrid scaffold, respectively. On bare PLGC fibers, cells were found aligned to the direction polymer fibers only. On the hybrid scaffold, cells were found in all directions, and across the fibers as well. Scale bar = 100μm.

Results

Development of a biodegradable hybrid scaffold

The soft, smooth texture and gross appearance of the electrospun PLGC scaffold (Fig. 1A) seemed favorable for skin applications. Electrospinning was successful and formed uniform-sized polymer fibers that were aligned in parallel (Fig. 1B). Average fiber diameter of 5.45 ± 0.64 μm was estimated using Image J software. The deposition of the biomimetic matrix to produce the hybrid scaffold showed effective development of a fragile fibrin network (Fig. 1D). Chemical evidence of matrix deposition is shown in Fig. 1E. The matrix was stable after lyophilization and could be suspended in the culture medium without delamination for growing cells *in vitro*. Water transmission potential of the scaffold was found to be promising (Fig. 2A). There was significant difference in the percentage swelling between bare and hybrid scaffolds—the former was 160 ± 9%, and the latter, 400 ± 42% (Fig. 2B).

Fibroblast growth on scaffolds

Within 7 d of culture, better cell growth was observed on the hybrid scaffold (Fig. 3A, B). The depth-coded projection of Z-stack images demonstrated migration of cells into the internal layers of the hybrid scaffold (Fig. 3E). By 28 d, all the fibers were covered by a sheet of fibroblasts (Fig. 3D), but in the case of bare PLGC, the polymer fibers were visible (Fig 3C). Cell migration from the hybrid scaffold was similar to that during skin explant culture (Fig. 3F). Quantitatively, ^{3}H-thymidine uptake showed exponential proliferation on the hybrid scaffolds as compared to the bare scaffolds (Fig. 4A). Qualitatively, more phalloidin-stained actin was evident

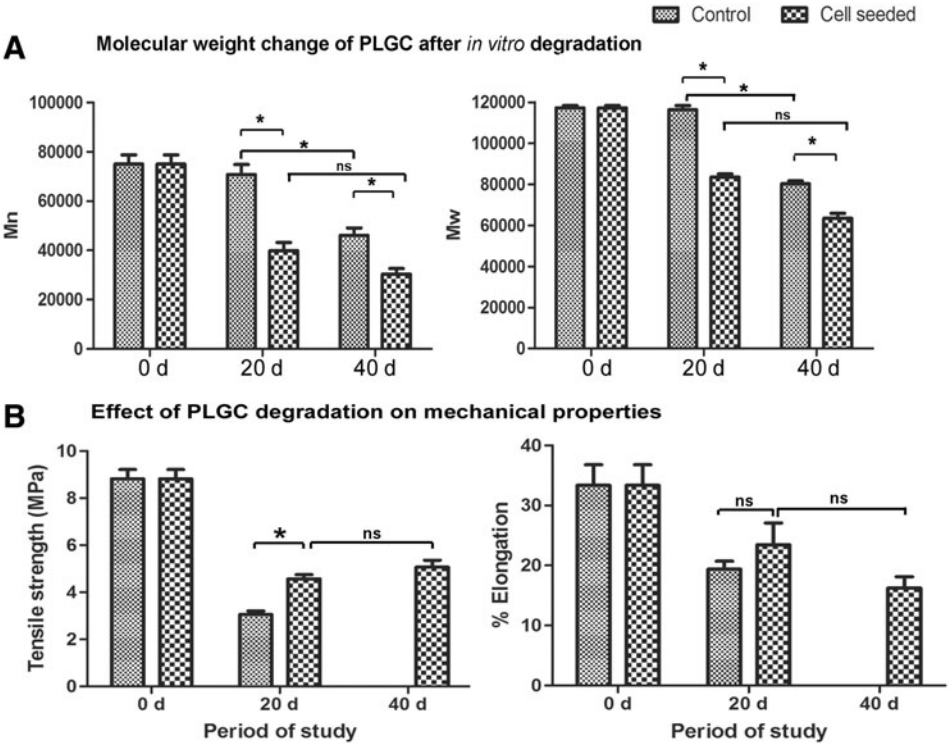

FIG. 5. Data on *in vitro* degradation of scaffold. **(A)** Change in molecular weight (weight average [Mw] and number average [Mn]) of polymer suspended in culture medium with or without fibroblast after different periods. **(B)** Tensile strength and percent elongation of hybrid scaffolds suspended in culture medium with or without fibroblast after different periods. Elongation was higher for cell-grown samples but was not statistically significant. Mechanical testing of cell-free scaffolds was not possible after 40 d of immersion in the medium because they were found to have lost the required dimension due to shrinkage. Data presented is average ± SD ($n = 5$). *$p < 0.05$. The periods of analysis are marked in the x-axis.

on the hybrid scaffold (Fig. 4B). Analysis using ESEM, ^{3}H thymidine uptake and actin distribution suggested that the biomimetic matrix enhanced fibroblast growth.

Mechanical properties of cell-grown scaffolds

The scaffold patches without cells shrunk over time when immersed in the medium, while the cell-grown scaffolds maintained their shape and dimension. Polymer degradation was evident from the reduction in both Mw and Mn by 20 d and 40 d, more significantly in the cell grown scaffolds (Fig. 5A, B). However, the tensile strength of the cell-grown scaffolds was significantly high as compared to that of cell-free ones on 20 d (Fig. 5C); by 40 d, in spite of progression in polymer breakdown which resulted in the reduction in Mn and Mw, the tensile strength was steady (Fig. 5B vs. Fig. 5D).

The immunostaining of the decellularized scaffold after 20 d of cell culture showed uniform deposition of collagen and elastin on the hybrid scaffold (Fig. 6B, D), but not much on the bare scaffold (Fig. 6A, C); both collagen and elastin deposition was three times more on the hybrid scaffold as compared with the bare scaffold by 20 d (Fig. 6C, D). No phenomenal change in ECM deposition was seen between 20 d and 40 d.

In vivo *scaffold degradation*

After 20 d and 40 d of implantation, Mn decreased to ~68% and 36%, respectively, and Mw decreased to about 72% and 59%, respectively (Fig. 7). Thus, the *in vitro* degradation of cell-grown scaffolds and *in vivo* degradation of bare scaffolds showed comparable outcomes.

Discussion

This study attempted to develop *in vitro* engineered dermal-like tissue with good biological and mechanical properties. Synthetic biodegradable polymers show great potential in tailoring their mechanical properties and degradation kinetics to suit specific needs.[4,5] The terpolymer used in the current study does not release any toxic component upon biodegradation. Ideally, nano- and micro-architectural

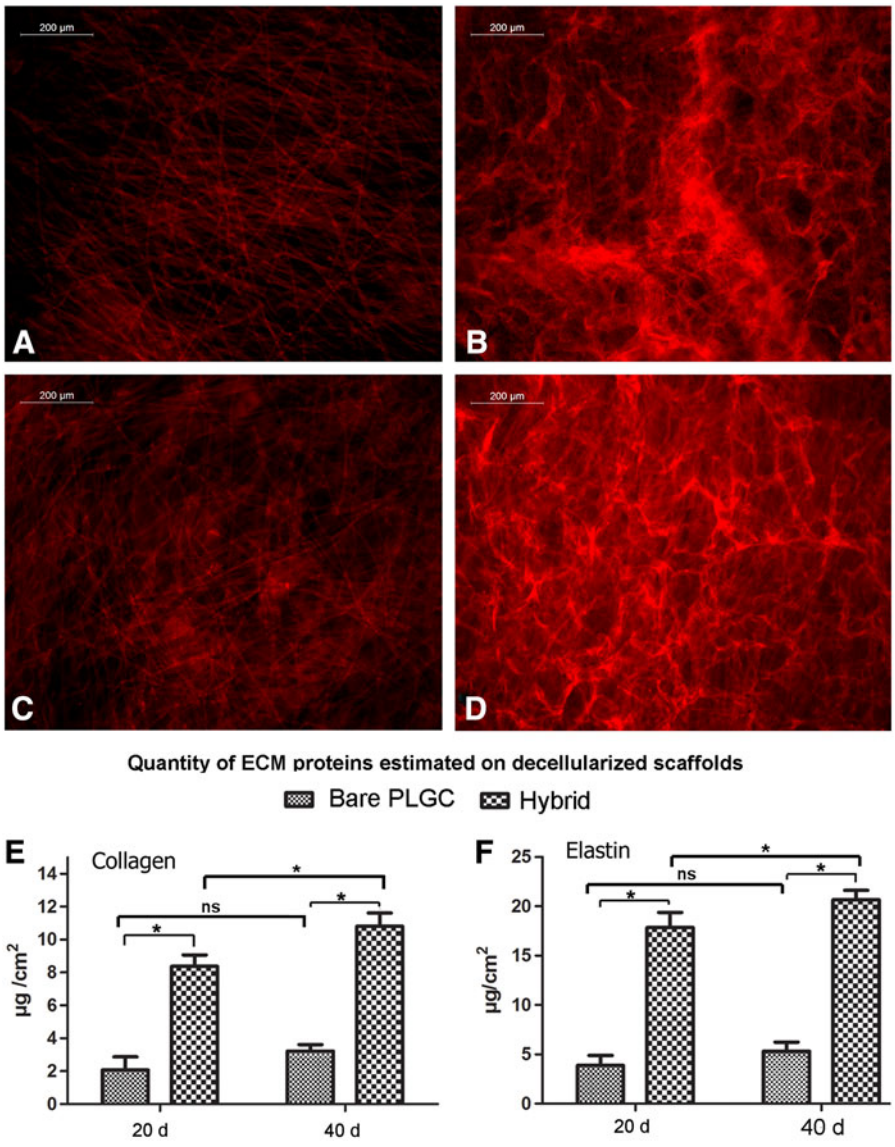

FIG. 6. Qualitative and quantitative analysis of extra cellular matrix (ECM). **(A, B)** Representative fluorescent images of elastin stained decellularized bare PLGC scaffold and hybrid PLGC scaffolds after 20 days of fibroblast culture. **(C, D)** Representative fluorescent images of collagen stained decellularized bare PLGC scaffold and hybrid PLGC scaffolds 20 d of fibroblast culture. **(E, F)** Quantity of collagen and elastin estimated on decellularized bare and hybrid scaffolds after 20 d and 40 d of fibroblast culture. Data presented is average ± SD, ($n = 3$). *$p < 0.05$.

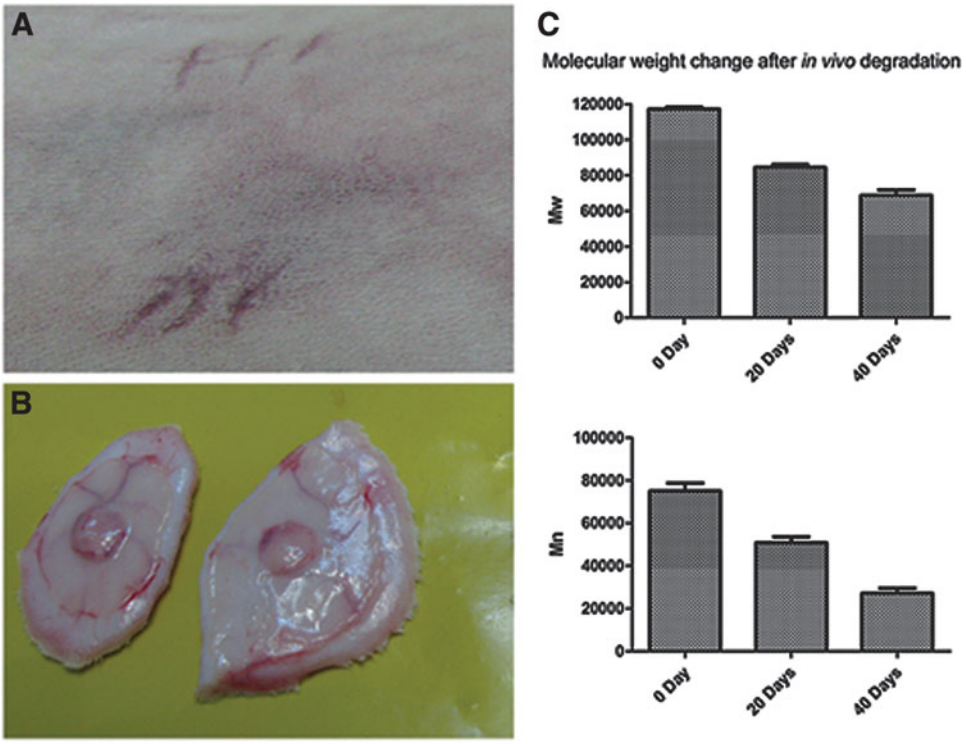

FIG. 7. Representative images of *in vivo* degradation study. **(A)** Rabbit skin after subcutaneous implantation of PLGC scaffolds. **(B)** Explanted skin patch with scaffold after 20 d of implantation. **(C)** Graphical representation of Mn and Mw of scaffolds before and after two periods of implantation. Data presented is average ± SD, ($n = 4$).

fibers of electrospun scaffolds with spacial interconnectivity should mimic the normal ECM-like architecture of tissue and possess properties such as efficient nutrient transport, controlled evaporative water loss, enhanced fluid drainage, oxygen permeability, and efficient cellular response.[16,21] The polymer scaffold is expected to provide mechanical support, but the tissue remodeling requires appropriate signals, which is why the hybrid scaffold in this study was developed by incorporating a biomimetic fibrin composite with PLGC.

Another advantage of the porous nature of the scaffold is good WVTR. Water vapor transmission rate for injured skin can range from $279 \pm 26\,g \cdot m^{-2} \cdot day^{-1}$ for first-degree burns to $5138 \pm 202\,g \cdot m^{-2} \cdot day^{-1}$ for a granulating wound.[23] It has been recommended that WVTR of 2000–2500 $g \cdot m^{-2} \cdot day^{-1}$ would provide an adequate level of moisture without wound dehydration. The values obtained for the scaffold developed in this study fall in the mid-range of loss from injured skin.[23] Though there is a reduction in pore volume and WVTR upon fibrin composite deposition, the values are within the recommended range. The water absorption ability of the scaffold reflects its capability to hold aqueous medium, which is necessary for cell growth and wound healing.[24,25] In this study, the hybrid scaffold exhibited significantly higher (2.5 times) swelling capacity than the bare scaffold. This increase in the swelling ratio of the hybrid scaffold may have been contributed mainly by the HA that was added to the biomimetic matrix. A moist environment enhances cell migration and chemokine mobility across the wound area resulting in increased epithelialization and reduced scarring.[26] Therefore, this scaffold by itself may enhance wound healing if implanted to guide tissue regeneration.

In *in vitro* conditions, there was not only significantly high cell growth on the hybrid scaffold, but the fibroblast were induced to synthetic phenotype, which caused further ECM deposition. When the construct was transferred to a fresh culture dish after fibroblast culture for 28 d on the hybrid scaffold, sprouting and migration of cells from the scaffold into the neighboring area suggested the migration/proliferation potential of these cells. Such migration of cells into the wounded tissue may help in a better and faster integration of the construct with the neighboring tissue after construct transplantation.

Higher collagen and elastin deposition on the hybrid scaffold is a consequence of better cell survival and growth. Pankajakshan et al. showed that endothelial cells, when grown for 10 d on fibrin matrix, enhanced synthesis and deposition of elastin and collagen.[27] In the current study, there was no remarkable difference in collagen and elastin deposition between 20 d and 40 d of the fibroblast culture, which suggested autoregulation. Therefore, cells that are grown are unlikely to turn into fibrotic phenotype with excessive deposition of collagen. This may be due to modulation of cell growth by HA, as its role in regulating proliferation and cellular activity such as synthesis of collagen by fibroblasts has been reported.[28] Therefore, the incorporation of HA in the fibrin composite may have additional benefits for controlled ECM deposition, which would increase mechanical strength while providing suppleness to the regenerated tissue.

The cell-grown scaffolds showed more physical stability, but the polymer backbone degraded at a faster rate than those without cells. Probably, the proteases released from cells influenced degradation of polymer chains, which resulted in the reduction of Mw and Mn. The stable mechanical property of the cell-grown scaffold seen in this study may be attributed to the ECM produced upon fibroblast culture. Tensile strength of human skin ranges between 3 and14 MPa.[29] Poor mechanical properties and rapid scaffold degradation can cause graft instability and handling difficulty. The hybrid scaffold developed in this study exhibited promising

tensile strength (8.82 ± 0.87 MPa). Literature suggests that fibroblasts are capable of degrading electrospun polymer fibers through enzymatic hydrolysis.[30] Well-spread fibroblasts produce stress fibers, which may accelerate enzymatic degradation.[31] Poor tensile strength may be the outcome of accelerated polymer degradation. In this study, the tensile strength and elongation of scaffolds on which fibroblasts were cultured were significantly higher than in the control scaffolds (incubated without seeding fibroblasts). The most probable reason for increased tensile strength is support from the newly formed ECM. The deposited ECM seems to have compensated for the scaffold degradation-dependant loss of tensile strength. So a tissue engineering experience where the effect of scaffold degradation on mechanical strength is balanced due to tissue generation holds promise. By analyzing *in vivo* degradation upon implantation, a clearer picture of *in vivo* effect was obtained. Similar to *in vitro* degradation of the cell-seeded scaffold, the *in vivo* degradation rate of the scaffold was also evident on 20 d with further degradation by 40 d of implantation. The slightly higher initial *in vivo* degradation rate as compared to *in vitro* degradation rate may be due to the action of inflammatory cells. We conclude that the mechanical strength of the degraded polymer scaffold was maintained by the ECM deposited by fibroblasts. This is an ideal tissue engineering model for constructing skin substitutes.

Acknowledgments

The authors acknowledge Dr. K. Radhakrishnan, Director of Sree Chitra Tirunal Institute for Medical Sciences and Technology (SCTIMST) and Dr. G.S. Bhuvaneshwar, Head of Biomedical Technology Wing, SCTIMST, for their encouragement and support. We thank Ms. S. Priyanka and Mr. S. Ranjith for providing us with human fibrinogen and thrombin. We would like to acknowledge the project fund from the Council of Scientific and Industrial Research (CSIR), Government of India, and also the individual fellowship support to Mr. Renjith P. Nair from CSIR.

Author Disclosure Statement

No competing financial interests exist.

References

1. Papini R. Management of burn injuries of various depths. BMJ. 2004;329:158–160.
2. Shevchenko RV, James SL, James SE. A review of tissue-engineered skin bioconstructs available for skin reconstruction. J R Soc Interface. 2010;7:229–258.
3. Garcia-Gareta E, Ravindran N, Sharma V, et al. A novel multiparameter in vitro model of three-dimensional cell ingress into scaffolds for dermal reconstruction to predict in vivo outcome. Biores Open Access. 2013;2:412–420.
4. Zhong SP, Zhang YZ, Lim CT. Tissue scaffolds for skin wound healing and dermal reconstruction. Wiley Interdiscip Rev Nanomed Nanobiotechnol. 2010;2:510–525.
5. Moura LIF, Dias AMA, Carvalho E, et al. Recent advances on the development of wound dressings for diabetic foot ulcer treatment—A review. Acta Biomater. 2013;9:7093–7114.
6. Metcalfe AD, Ferguson MW. Bioengineering skin using mechanisms of regeneration and repair. Biomaterials. 2007; 28:5100–5113.
7. Nair RP, Krishnan LK. Identification of p63+keratinocyte progenitor cells in circulation and their matrix-directed differentiation to epithelial cells. Stem Cell Res Ther. 2013; 4:38.
8. Wang X, You C, Hu X, et al. The roles of knitted mesh-reinforced collagen-chitosan hybrid scaffold in the one-step repair of full-thickness skin defects in rats. Acta Biomater. 2013;9:7822–7832.
9. Hongxu L,Oh HH, Naoki K, et al. PLLA–collagen and PLLA–gelatin hybrid scaffolds with funnel-like porous structure for skin tissue engineering. Sci Technol Adv Mater. 2012;13:064210.
10. Campos DM, Gritsch K, Salles V, et al. Surface entrapment of fibronectin on electrospun PLGA scaffolds for periodontal tissue engineering. BioRes Open Access. 2014;3:117–126.
11. Pankajakshan D, Philipose LP, Palakkal M, et al. Development of a fibrin composite-coated poly(ε-caprolactone) scaffold for potential vascular tissue engineering applications. J Biomed Mater Res B Appl Biomater. 2008;87: 570–557.
12. Kumar TR, Krishnan LK. A stable matrix for generation of tissue-engineered nonthrombogenic vascular grafts. Tissue Eng. 2002;8:763–770.
13. Ahmed TA, Dare EV, Hincke M. Fibrin: a versatile scaffold for tissue engineering applications. Tissue Eng Part B Rev. 2008;14:199–215.
14. Laurens N, Koolwijk P, de Maat MP. Fibrin structure and wound healing. J Thromb Haemost. 2006;4:932–939.
15. Anilkumar TV, Muhamed J, Jose A, et al. Advantages of hyaluronic acid as a component of fibrin sheet for care of acute wound. Biologicals. 2011;39:81–88.
16. Wang X, Ding B, Li B. Biomimetic electrospun nanofibrous structures for tissue engineering. Mater Today. 2013;16: 229–241.
17. Khil MS, Cha DI, Kim HY, et al. Electrospun nanofibrous polyurethane membrane as wound dressing. J Biomed Mater Res B Appl Biomater. 2003;67:675–679.
18. Boudriot U, Dersch R, Greiner A, et al. Electrospinning Approaches toward scaffold engineering—A brief overview. Artif Organs. 2006;30:785–792.
19. Srisaard M, Molloy R, Molloy N, et al. Synthesis and characterization of a random terpolymer of L-lactide, -caprolactone and glycolide. Polym Int 2001;50:891–896.
20. Mi FL, Shyu SS, Wu YB, et al. Fabrication and characterization of a sponge-like asymmetric chitosan membrane as a wound dressing. Biomaterials. 2001;22:165–173.
21. Pankajakshan D, Krishnan VK, Krishnan LK. Vascular tissue generation in response to signaling molecules integrated with a novel poly(ε-caprolactone)–fibrin hybrid scaffold. J Tissue Eng Regen Med. 2007;1:389–397.
22. Choi YC, Choi JS, Kim BS, et al. Decellularized extracellular matrix derived from porcine adipose tissue as a xenogeneic biomaterial for tissue engineering. Tissue Eng Part C Methods. 2012;18:866–876.
23. Lamke LO, Nilsson GE, Reithner HL. The evaporative water loss from burns and the water-vapour permeability of grafts and artificial membranes used in the treatment of burns. Burns. 1977;3:159–165.
24. Luangbudnark W, Viyoch J, Laupattarakasem W, et al. Properties and biocompatibility of chitosan and silk fibroin blend films for application in skin tissue engineering. Scientific World Journal. 2012;2012:697201. Available online at http://dx.doi.org/10.1100/2012/697201.

25. Yamaguchi Y, Kubo T, Murakami T, et al. Bone marrow cells differentiate into wound myofibroblasts and accelerate the healing of wounds with exposed bones when combined with an occlusive dressing. Br J Dermatol. 2005;152:616–622.
26. Junker JP, Kamel RA, Caterson EJ, et al. Clinical impact upon wound healing and inflammation in moist, wet, and dry environments. Adv Wound Care. 2013;2:348–356.
27. Pankajakshan D, Krishnan LK. Design of fibrin matrix composition to enhance endothelial cell growth and extracellular matrix deposition for in vitro tissue engineering. Artif Organs. 2009;33:16–25.
28. Mast BA, Diegelmann RF, Krummel TM, et al. Hyaluronic acid modulates proliferation, collagen and protein synthesis of cultured fetal fibroblasts. Matrix. 1993;13:441–446.
29. Jansen LH, Rottier PB. Comparison of the mechanical properties of strips of human abdominal skin excised from below and from above the umbilic. Dermatology. 1958;117:252–258.
30. Pan H, Jiang H, Chen W. The biodegradability of electrospun dextran/PLGA scaffold in a fibroblast/macrophage co-culture. Biomaterials. 2008;29:1583–1592.
31. Pan H, Jiang H, Chen W. Interaction of dermal fibroblasts with electrospun composite polymer scaffolds prepared from dextran and poly lactide-co-glycolide. Biomaterials. 2006;27:3209–3220.

Address correspondence to:
Lissy K. Krishnan, PhD
Thrombosis Research Unit
Biomedical Technology Wing
Sree Chitra Tirunal Institute for Medical Sciences and Technology
Trivandrum 695012
India

E-mail: lissykk@sctimst.ac.in

Abbreviations Used

PLGC = poly(lactide-glycolide-caprolactone)
ECM = extracellular matrix
HA = Hyaluronic acid
HBSS = Hanks' Balanced Salt Solution
GPC = gel permeation chromatography
CPCSEA = Committee for the Purpose of Control and Supervision on Experiments on Animals